# HIGH-ORDER COMPACT SCHEMES FOR PLASMA WAVE SIMULATION*

**M. D. White**ξ
*Ohio Aerospace Institute & Air Force Research Laboratory,*
*WPAFB, Ohio, 45433 USA*

*Abstract*

A high-order finite-difference code has been developed with the ability to simulate waves in plasmas coupling Maxwell Equations with fluid species equations. Originally developed to examine the radio blackout problem, the code utilizes $6^{th}$-order finite-differences with $10^{th}$-order filters in space and $4^{th}$-order Runge-Kutta in time in order to minimize the number of grid points while retaining the fidelity of the solution. The code also uses multiple overlapping grids allows for solving complex configurations in parallel.

## I. INTRODUCTION

Over the past few years the Air Force has been interested in development of high fidelity simulation capabilities to investigate the long standing problem of radio blackout during reentry. To address this issue, a high-order finite-difference code has been developed by the Air Vehicles Branch of the Air Force Research Laboratory which can simulate electromagnetic plasma waves.[1-3] The current configuration requires that the plasma be generated by another source, and the background electron density and temperature are fed into *OHMS* (Overset High-order Maxwell Solver) which solves the propagation problem.[2-3]

## II. METHODOLOGY

### *A. Equation set*

The equations for plasma propagation by the electrons can be written as:

$$\epsilon_0 \partial_t \mathbf{E}_1 + \mathbf{J}_{e,1} - \nabla \times (\mathbf{B}_1/\mu_0) = 0$$

$$\partial_t \mathbf{B}_1 + \nabla \times \mathbf{E}_1 = 0$$

$$\partial_t n_{e,1} - \frac{\nabla \cdot \mathbf{J}_{e,1}}{e} = 0$$

$$\partial_t \mathbf{J}_{e,1} = \left(\frac{e^2 n_e}{m_e}\right)\mathbf{E}_1 + e\frac{\gamma_e R T_e \nabla n_{e,1}}{m_e} - \nu_e \mathbf{J}_{e,1}$$

where the subscript "1" indicates a perturbation of the variable. In non-dimensional form, the equations reduce to [3]:

$$\partial_t \mathbf{E} + \mathbf{J}_e - \nabla \times \mathbf{B} = 0$$

$$\partial_t \mathbf{B} + \nabla \times \mathbf{E} = 0$$

$$\partial_t \varsigma_e - \nabla \cdot \mathbf{J}_e = 0$$

$$\partial_t \mathbf{J}_e = \Omega_p^2 n_{e,0}\,\mathbf{E} + \beta_{th}^2 T_{e,0} \nabla \varsigma_e - \nu_e \mathbf{J}_e$$

where the perturbation subscript "1" has been suppressed, $\boldsymbol{\Omega}_p$ is the electron plasma frequency multiplied by the time scale, $\varsigma_e$ is the perturbation electron density multiplied by its charge and $\boldsymbol{\beta}_{th}$ is the ratio of the root-mean-squared molecular velocity of the electrons based on the reference temperature ($T_{e,ref}$) divided by the speed of light in vacuum. Thus, the code solves 10 equations needing 12 variables of storage.

### *B. Computational Method*

The *OHMS* code uses $6^{th}$-order finite-difference modeling in generalized curvilinear coordinates:[3-5]

$$\alpha \frac{\partial F_{j-1}}{\partial \xi_i} + \frac{\partial F_j}{\partial \xi_i} + \alpha \frac{\partial F_{j+1}}{\partial \xi_i} = a\left(\frac{F_{j+1} - F_{j-1}}{2\Delta \xi_i}\right) + b\left(\frac{F_{j+1} - F_{j-1}}{4\Delta \xi_i}\right)$$

for any variable $F$ at point $j$ being differenced in the $\xi_i$ direction. The order of accuracy is satisfied by restricting the coefficients:

$$2^{nd}\ order: \quad (1 + 2\alpha) = (a + b)$$

$$4^{th}\ order: \quad \alpha = (a + 4b)/6$$

$$6^{th}\ order: \quad \alpha/12 = (a + 16b)/5!$$

* Work supported by Dr. Nachman of the Air Force Office of Scientific Research under contract FA8650-04-2-3445
ξ email: Michael.White@wpafb.af.mil

# Report Documentation Page

*Form Approved*
*OMB No. 0704-0188*



| | | |
|---|---|---|
| 1. REPORT DATE **JUN 2007** | 2. REPORT TYPE **N/A** | 3. DATES COVERED **-** |
| 4. TITLE AND SUBTITLE **High-Order Compact Schemes For Plasma Wave Simulation** | | 5a. CONTRACT NUMBER |
| | | 5b. GRANT NUMBER |
| | | 5c. PROGRAM ELEMENT NUMBER |
| 6. AUTHOR(S) | | 5d. PROJECT NUMBER |
| | | 5e. TASK NUMBER |
| | | 5f. WORK UNIT NUMBER |
| 7. PERFORMING ORGANIZATION NAME(S) AND ADDRESS(ES) **Ohio Aerospace Institute & Air Force Research Laboratory, WPAFB, Ohio, 45433 USA** | | 8. PERFORMING ORGANIZATION REPORT NUMBER |
| 9. SPONSORING/MONITORING AGENCY NAME(S) AND ADDRESS(ES) | | 10. SPONSOR/MONITOR'S ACRONYM(S) |
| | | 11. SPONSOR/MONITOR'S REPORT NUMBER(S) |

12. DISTRIBUTION/AVAILABILITY STATEMENT
**Approved for public release, distribution unlimited**

13. SUPPLEMENTARY NOTES
**See also ADM002371. 2013 IEEE Pulsed Power Conference, Digest of Technical Papers 1976-2013, and Abstracts of the 2013 IEEE International Conference on Plasma Science. IEEE International Pulsed Power Conference (19th). Held in San Francisco, CA on 16-21 June 2013., The original document contains color images.**

14. ABSTRACT
**A high-order finite-difference code has been developed with the ability to simulate waves in plasmas coupling Maxwell Equations with fluid species equations. Originally developed to examine the radio blackout problem, the code utilizes 6th-order finite-differences with 10th-order filters in space and 4th-order Runge-Kutta in time in order to minimize the number of grid points while retaining the fidelity of the solution. The code also uses multiple overlapping grids allows for solving complex configurations in parallel.**

15. SUBJECT TERMS

| 16. SECURITY CLASSIFICATION OF: | | | 17. LIMITATION OF ABSTRACT | 18. NUMBER OF PAGES | 19a. NAME OF RESPONSIBLE PERSON |
|---|---|---|---|---|---|
| a. REPORT **unclassified** | b. ABSTRACT **unclassified** | c. THIS PAGE **unclassified** | **SAR** | **4** | |

**Standard Form 298 (Rev. 8-98)**
Prescribed by ANSI Std Z39-18

The resulting discrete equations for the partial derivatives are solved implicitly using a tridiagonal solver. The effective wavenumbers resulting from explicit and compact differencing is shown in figure 1. Added to the graph is the equivalently scaled spectral response of Finite Difference Time Domain (FDTD).

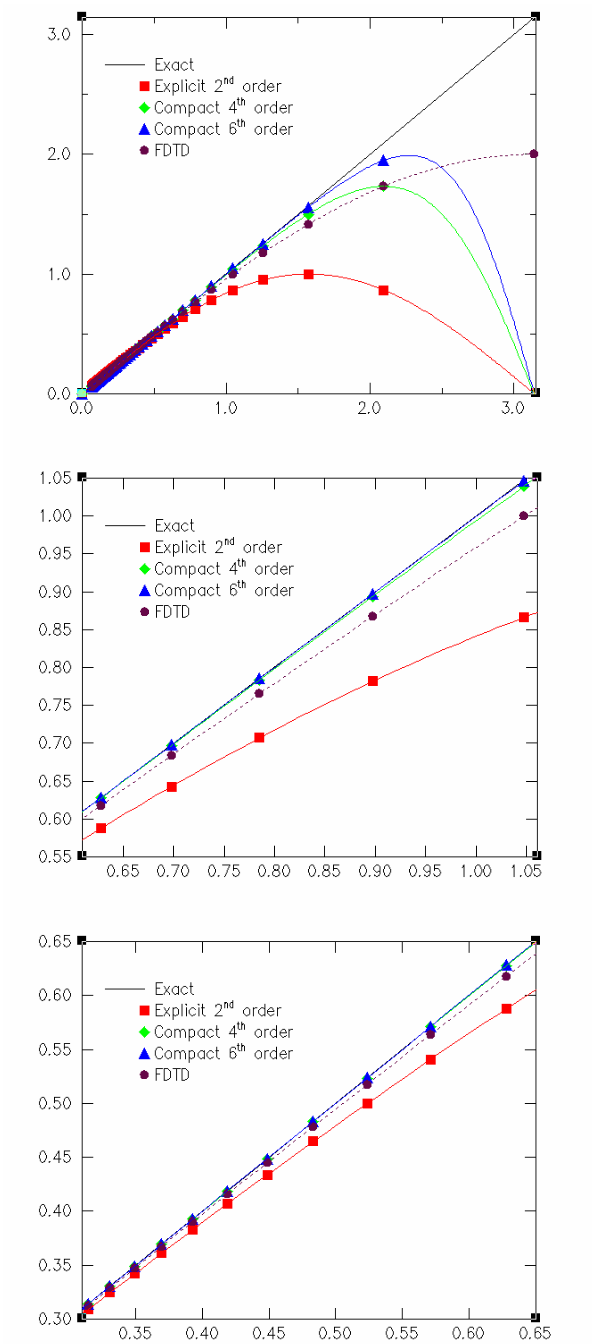


**Figure 1**. Reduced wavenumber for different schemes. Top: Wavenumber kΔx vs effective wavenumber k'Δx for λ = 2Δ to ∞. Middle: 10 to 6 points per wavelength. Bottom: 20 to 10 points per wavelength.

### *C. Filtering*

Filtering is utilized both for stability [4,5] and for the absorbing boundary conditions[6]. The filters are designed so that wavelengths λ = 2Δ are completely eliminated while long wavelengths are unattenuated. The basic filter equation is solved using a tridiagonal solver:

$$\alpha_f \hat{F}_{j-1} + \hat{F}_j + \alpha_f \hat{F}_{j+1} = \sum_{n=0}^{N} \frac{a_n}{2}\left(F_{j+n} + F_{j-n}\right)$$

where for 10$^{th}$ order: a0 = (193 + 126 $\alpha_f$)/256, a1 = (105 + 302 $\alpha_f$)/256, a2 = -15(1 - 2 $\alpha_f$)/64, a3 = 45 (1 - 2 $\alpha_f$)/512, a4 = -5(1-2 $\alpha_f$)/256, a5 = (1-2 $\alpha_f$)/512, and $\alpha_f$ varies from 0 to 0.499 (typical values are 0.3 to 0.49). The transfer function is given by:

$$\mathrm{T}(\omega) = \frac{\sum_{n=0}^{N} a_n \cos(n\omega)}{1 + 2\alpha_f \cos(\omega)}$$

where ω = 2 π Δ / λ. Figure 2 for different values of $\alpha_f$.

### *D. Chimera*

*OHMS* has the capability for multiple overlapping grids (Chimera) to be solved in parallel. The grid communication is given via Lagrangian interpolation.[7,8] The Chimera paradigm allows for the easy implementation of the scattered field/total field interface by defining each grid as either a scattered or total field grid. The incident fields can then be added to or subtracted from the interpolated values during the message passing.[3]

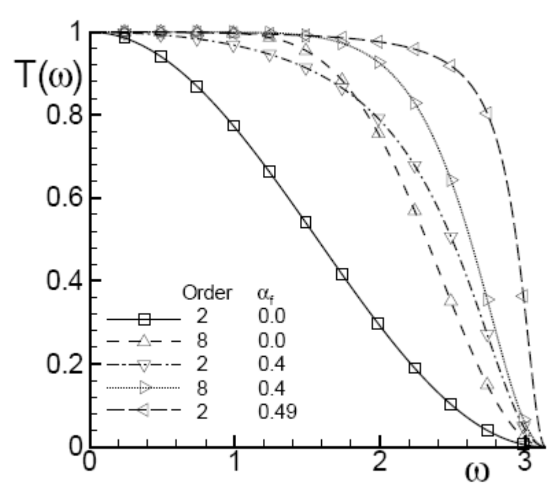


**Figure 2**. Transfer function for filter orders 2-8 for various values of $\alpha_f$.

## III. RESULTS

Propagation of a signal from an horn antenna was simulated using a background plasma generated by a non-equilibrium re-entry code developed by Josyula and Bailey.[9] For the given antenna location, the maximum electron temperature was T = 0.1 eV. At this temperature, no effect was seen by the addition of the electron temperature – indicating that for most re-entry problems, solving an auxiliary ordinary differential equation for the current is all that is necessary. While removing only a single equation, the number of variable storage is reduced by 2 and 25 fewer tridiagonal solves are needed per time step. To see the effect of the extra equation, the reference electron temperature was artificially raised to 100 eV and 5 keV. As seen in figure 3, there is almost no change in the electric field from 0.1 to 100 eV. At 5 keV there is a noticeable change in the field radiating from the horn. In this case, the signal frequency is below the peak plasma frequency for the electron density distribution causing the wave to be highly attenuated. Looking at the current a few grid points above the horn aperture in figure 4, there was no noticeable difference in the current for 0.1 to 100 eV reference temperature. As seen by the instantaneous E field in figure 5, the effect of the plasma temperature is greatest nearest the surface of the vehicle, and its influence drops off as the distance increases.

## IV. SUMMARY

A high-order finite-difference methodology has been presented for simulating electromagnetic plasma waves in complex configurations. For most reentry problems, the effect of electron temperature will likely be confined to near the vehicle body and appears to be negligible in terms of the radio blackout problem. While not currently implemented, the addition of the $\mathbf{J}_e \times \mathbf{B}_0$ term is straight forward, requiring only three more variables of storage.

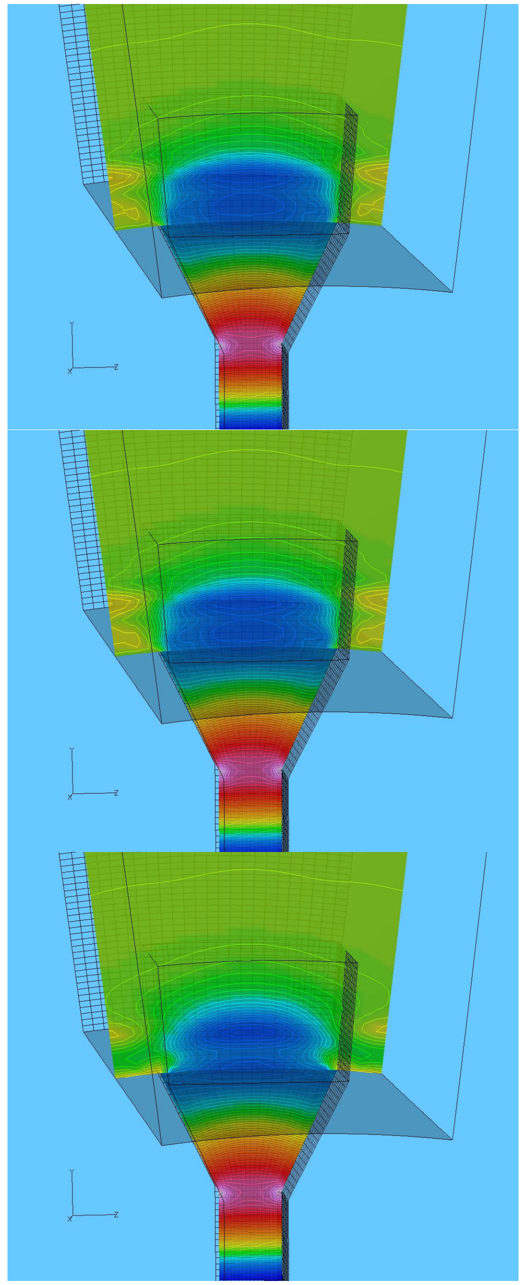

**Figure 3**. Effect of the electron temperature on the wave propagation from the horn antenna. Top: $T_{e,ref}$ = 0.1 eV. Center: $T_{e,ref}$ = 100 eV. Bottom: $T_{e,ref}$ = 5.0 keV.

## V. REFERENCES


[1] M. D. White, "Simulation of Communications Through a Weakly Ionized Plasma for a Re-entry Vehicle at Mach 23.9", 2005 IEEE Antennas and Propagation Society International Symposium, Washington, DC, July 3-8, 2005, vol. 4B, pp. 418-421

[2] M. D. White and S. E. Sherer, "High-Order Simulation of Communication Through a Weakly Ionized Plasma for Re-entry Vehicles", 44th AIAA Aerospace Sciences Meeting and Exhibit, Reno, Nevada, Jan. 9-12, 2006

[3] M. D. White, "Communication Through a Non-Equilibrium Hypersonic Boundary Layer for Re-entry Vehicles", 45th AIAA Aerospace Sciences Meeting and Exhibit, Reno, Nevada, Jan. 8-11, 2006.

[4] Shang, J. S., "Higher-Order Compact-Difference Schemes for Time-Dependent Maxwell Equations," *J. Comput. Phys.*, Vol. 153, 1999, pp. 312 – 333.

[5] Gaitonde, D. and Visbal, M., \High-Order Schemes for Navier-Stokes Equations: Algorithm and Implementation into FDL3DI," *Tech. Rep. AFRL-VA-WP-TR-1998-3060*, Air Force Research Labs, 1998

[6] White, M. D. and Visbal, M. R., \Using Filters to Design Absorbing Boundary Conditions for High-Order CEM," *IEEE Trans. Magn.*, Vol. 40, No. 2, Mar 2004, pp. 961-964.

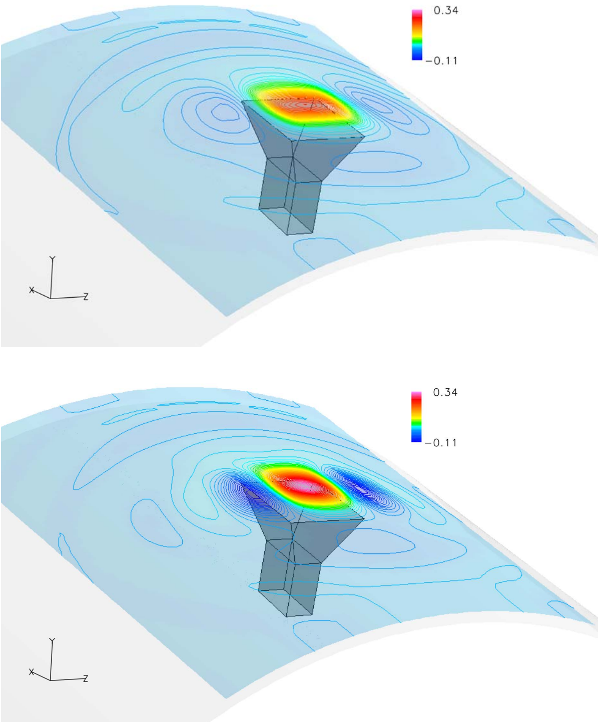


**Figure 4**. Contours of current above the horn antenna. Top: $T_{e,ref} = 0.1$ eV or 100 eV. Bottom: $T_{e,ref} = 5.0$ keV

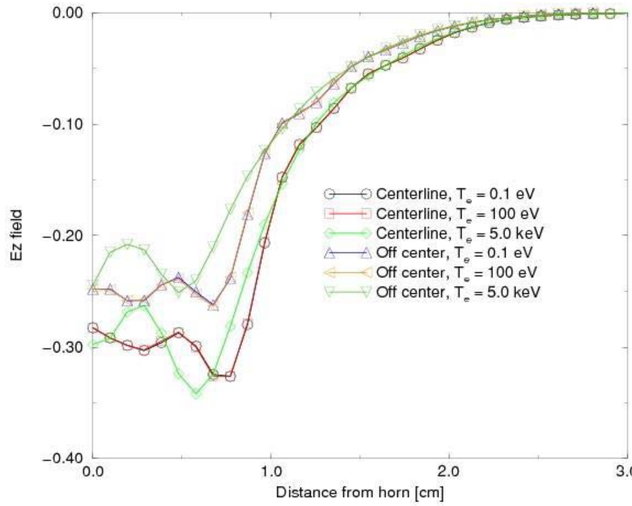


**Figure 5**. Effect of electron temperature on the electric field strength as it propagates from the horn.

[7] S. E. Sherer and J. N. Scott, "High-order compact finite-difference methods on general overset grids," *J. Comput. Phys.,* Vol. 210, 2005, pp. 459-496.

[8] S. E. Sherer and M. R. Visbal, "Time-Domain Scattering Simulations Using a High-Order Overset Grid Approach," 2005 Workshop on Computational Electromagnetics in Time-Domain (CEM-TD), Sept 12-14, 2005

[9] Josyula, E. and Bailey, W. F., "Governing Equations for Weakly Ionized Plasma Flowfields of Aerospace Vehicles," *J. Spacecraft and Rockets*, Vol. 40, No. 6, Nov-Dec 2003, pp. 845-857